STUDY ON MECHANICAL BEHAVIOR OF HYBRID MEMBER COMPOSED OF CEDAR-GLULAM TIMBER AND STEEL PLATE WITH FRICTION CONNECTOR

H. Sakata[1], M. Jokaku[2], S. Nakano[3], A. Tomimoto[4], Y. Nakamura[4]

[1] *Associate Professor, Structural Engineering Research Center, Tokyo Institute of Technology, Yokohama, Japan*
[2] *Takenaka Corporation (Former Graduate Student, Tokyo Institute of Technology), Japan*
[3] *Graduate Student, Tokyo Institute of Technology, Yokohama, Japan*
[4] *Manager, Nippon Steel Engineering Corporation, Japan*
Email: **hsakata@serc.titech.ac.jp**

ABSTRACT :

A hybrid member composed of a thin steel plate sandwiched between two glued-laminated cedar timber members has been developed and studied. The steel and timber parts were connected with shear-ring connectors and bolts. When using the shear-ring connector, the initial clearance between the shear-ring and the glulam timber needs to be wider to enable the hybrid member to be built up. Thus, the connectors were improved by introducing a friction joint. In this study, shear tests were conducted on the friction connectors, and axial compression tests were conducted on the hybrid members to determine the compression characteristics, and new estimation equations were proposed. The stiffness of hybrid members with friction connectors was higher than that of members with shear-ring connectors, and the former could be easily built up. The characteristics of these members were determined by shear tests and axial compression tests. It was thus possible to predict their axial compressive strength with sufficient accuracy by evaluating the shear strength and the shear stiffness of the connector by appropriately considering the connectors' characteristics.

KEYWORDS: Friction Connector, Hybrid Member, Alignment of Connector, Shear Stiffness of Connector, Estimation of Axial Strength

1. INTRODUCTION

1.1. Study Objectives and Background

The Authors have focused on the use of cedar to prevent buckling of steel plate, not as the main structural member. We have carried out experimental studies on methods of connecting cedar glulam timber and steel plate. As a result, they have developed a friction connection[1)] (Figure 1) that is better than the traditional shear-ring connection[2)] (Figure 2). We have also verified the shear stiffness of hybrid members using friction connectors, determined their mechanical behavior under axial compression, and demonstrated their effectiveness in controlling the buckling of steel plate[3), 4)]. Furthermore, we have proposed a method[3), 4)] for estimating the strength of these hybrid members. The method can be used to estimate the strength and identify the buckling mode of members by carrying out shear tests, axial compression tests. It is noted that multiple friction connectors could be used, although only a single one was used in previous studies.This report deals with shear tests conducted with multiple friction connectors placed at a single connection location of a glulam cedar-timber and steel plate member. It also presents the mechanical behavior of these connectors and the applicability of proposed equations to estimation of strength.

1.2. Hybrid Members

1.2.1 Composition of hybrid members

Figure 3 shows the hybrid members. It was assumed that they would be applied to the upper chord, which would be mainly in compression. Axial force propagated from the member end to the steel plate was further propagated to the cedar glulam timber via the connector. The cedar glulam timber stiffened the steel plate, thus inhibiting out-of-plane buckling.

1.2.2 Friction connector

Details of the connector for the cedar glulam timber and steel plate are shown in Figure 4. Thick-wall pipe of ϕ50 was forced into ϕ49.5 holes in the cedar glulam timber (Figure 4(a)). Steel plate was sandwiched between two plates of glulam timber such that the steel plate came in contact with the thick-wall pipe end. A high strength bolt was inserted into the thick-wall pipe and the plates were tightened(Figure 4(b)). The thick-wall pipe and steel plate were thus friction-connected and integrated with glulam timber. Zinc-rich coating was applied to the surfaces of steel plate and thick-wall pipe. The thick-wall pipe was configured as ϕ50h50 with an aspect ratio of 1[1]. Hereinafter, friction connector is called "connector".

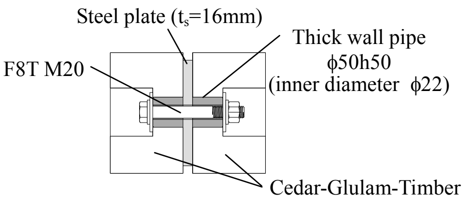

Figure 1 Cross Section with the Friction Connector

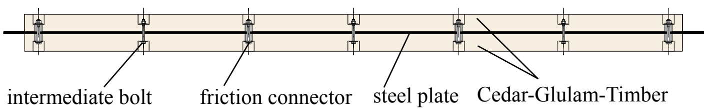

Figure 3 Hybrid Member

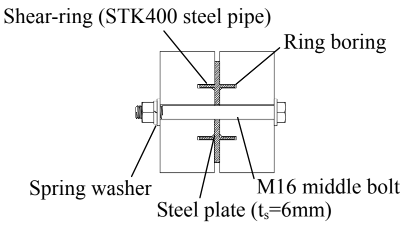

Figure 2 Cross Section with the Shear-ring

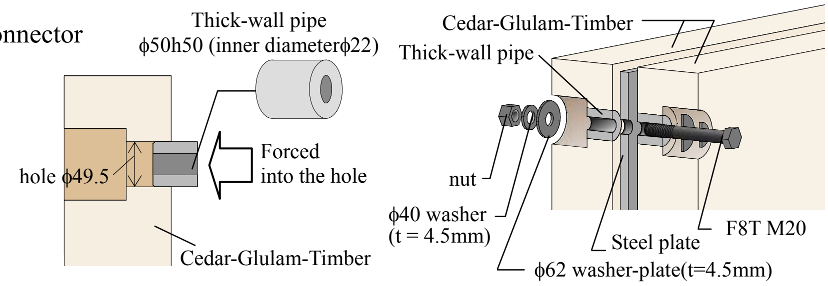

(a) Press Fitting of The Thick-Wall Pipe (b) Setting after Press Fitting

Figure 4 Setting of The Friction Connector

2. SHEAR TEST FOR FRICTION CONNECTOR

2.1. Test Piece

To obtain the shear behavior of the connector prior to the member tests, shear tests of the connector were carried out. The properties of the cedar glulam timber employed as the test piece, an outline of the test pieces and the connector layout, are shown in Tables 1 and 2 and Figure 5, respectively. The parameters were determined as thickness of cedar glulam timber, number of connectors, connector distance and loading direction. The tests were carried out using three test pieces each time. Thickness of glulam timber was denoted as h_w. Three thicknesses were tested: h_w = 50, 120 and 150mm. The number of connectors was categorized as Type c1: single connector and Type c2: two connectors placed the in loading direction and the loading–normal direction. In Type c2, the distance between connectors was denoted as r. Three distances were specified: r = 100, 150 and 200mm.

2.2. Loading Method and Measurement Plan

The loading method and measurement plan are shown in Figure 6. Monotonic compressive loading was carried out by pushing the connectors toward each other. Monotonic tensile loading was carried out for Type c1 (h_w = 50 and 120mm). The loading rate was held static at 0.5 mm/min. Displacement of the distance $\Delta 1$ between upper and lower steel plates and displacement of the distance $\Delta 2$ between the upper and lower connectors of the glulam timber were measured. Slip Δ per single connection surface is defined in Figure 6. To confirm no gap between the steel plate and thick-wall pipe, $\Delta 3$ was measured. Half of the load applied to the test pieces was defined as the shear force per single connection surface Q.

2.3. Results of Connector Shear Tests

The test results and relationship between shear force Q and slip Δ per single connection surface are shown in Table 2 and Figure 7, respectively. The shear stiffness at each load was determined as secant stiffness to the origin. The figure was taken as the average of the three test pieces. The difference between $\Delta 1$ and $\Delta 3$ was

Table 1 Material Property

Batch	Cedar-Glulam-Timber (E65-F225) laminate thickness : 32mm				
	Bending young Coef. kN/mm^2		Bending Stress N/mm^2		Water Content %
	Ewx-x	Ewy-y	x-x	y-y	
A	8.13	7.01	53.2	34.0	12.8
B	7.63	5.71	41.8	32.7	10.8

※x-x : load at a right angle to laminates, y-y : load parallel to laminates

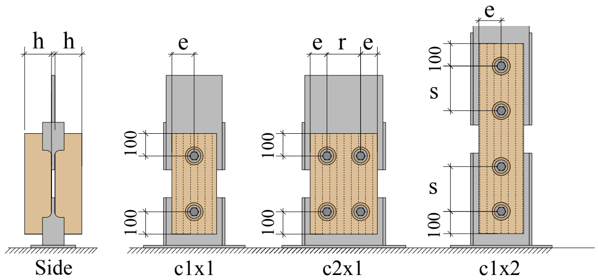

Figure 5 Layout of Friction Connectors

Table 2 Specimens for Connector Test

Name	Steel PL-t_s x b_s	Timber h_w x b_w	Distance (see Fig. 5) e=100	Batch	Maximum Shear Force per Single Connection Surface Qmax[kN]	Shear Stiffness per Single Connection Surface K_C [N/mm(x10^3)]			
h_w50c1x1		2 50x200	-	A	64.2		201		160
h_w120c1x1	PL-16x250	2 120x200	-	A	68.3	10kN	349	20kN	165
h_w150c1x1		2 150x200	-	B	72.1		329		190
r100h_w120c2x1	PL-16x350	2 120x300	r=100	B	133		263		223
r150h_w120c2x1	PL-16x400	2 120x350	r=150	B	136	20kN	429	40kN	270
r200h_w120c2x1	PL-16x450	2 120x400	r=200	B	134		346		245
s100h_w120c1x2			s=100	B	74.3		263		223
s200h_w120c1x2	PL-16x250	2 120x200	s=200	B	129	20kN	429	40kN	270
s300h_w120c1x2			s=300	B	124		346		245
h_w50c1x1-T	PL-16x250	2 50x200	-	B	26.8	10kN	91.6	20kN	70.7
h_w120c1x1-T		2 120x200	-	B	33.8		116		85.9

h_w : Thickness of Glulam-Timber
r : case of connectors set at right angles to the axis of the member
s : case of connectors set parallel to the axis of the member
Name - T : case of the tensile test
K_c : Secant Stiffness calculated with Average Result of Three Tests

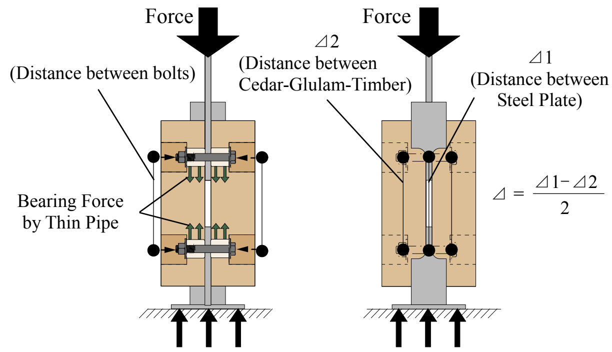

Loading Form which Each Connector Pressed

(a)Cross Section (b)Front Elevation

Figure 6 Loading Method and Measurement plan

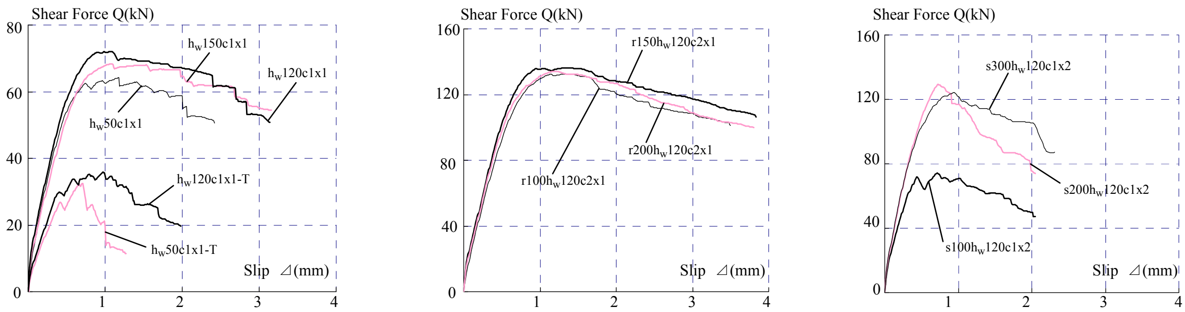

(a) Comparison of "h_w" and Loading Form (b) Comparison of "r" (c) Comparison of "s"

Figure 7 Relationship Between Shear Force Q and Slip Δ per Single Connection Surface

0.5mm or less up to the maximum shear force. Thus, no slip occurred up to maximum shear force. The shear stiffness at the connection location became one of critical element in defining the estimated strength of the hybrid members. In this respect, shear stiffness per parameter is compared as follows.

[Thickness of cedar glulam timber h_w] Results of compressive and tensile tests showed that the stiffness remained at the same level as long as the tests were within the elastic range regardless of the thickness, as shown in Figure 7(a). Accordingly, it is considered that the impacts of thickness on the shear stiffness of the connector are small.
[Connector distance r] As indicated in Figure 7(b), when stiffness and strength always remained at the same level, distance r between the connectors had no impact as long as r was over 100mm.
[Connector distance s] As shown in Figure 7(c), both stiffness and strength of the test piece with connector distance s = 100mm were lower than those with s = 200mm and 300mm. Test pieces with s = 200mm and 300mm showed similar stiffness and strength as long as they were within the elastic range.
[Connector number] The test piece with a single connector c1x1 was compared with that with two connectors placed in axial-normal direction c2x1. When a certain load level was applied, stiffness of test piece c2x1 was about 1.8 times that of test piece c1x1.

3. AXIAL COMPRESSION TEST

3.1. Specimen

An outline of the specimens and the mechanical properties of the steel plate are shown in Tables 3 and 4, respectively. The characteristics of the cedar glulam timber were the same as those of lot A, as shown in Table 1. The specimens are shown in Figure 8. The parameters were thickness h_w and width b_w of glulam timber, number of connecting locations for cedar glulam timber and steel plate using connectors, number of connectors at each connecting location, and thickness t_s and width b_s of foundation steel plate. The denotation of the specimens is shown in Figure 8. A flange was set at the steel plate end to increase local buckling load.

3.2. Loading Method and Measurement Plan

The test apparatus is shown in Figure 9. A monotonous compressive loading was applied using a 200kN hydraulic jack. Loading was stopped and unloading started when the load became lower than 80% of the axial strength was reached. Axial and out-of-plane displacements were measured. Strain gauges were attached to the right and left of the steel plate connector, as shown in Figure 10. Then, changes in axial force borne by the steel plate in the front and rear of the connector were estimated.

3.3. Results of Member Axial Compression Test

3.3.1 Axial force-axial deformation

The following were estimated from Equation (1): Euler buckling strength P_{cri} when glulam timber was regarded as having integrity, Euler buckling strength P_{crd} when glulam timber was regarded as individual members and Euler buckling strength P_e of the steel plate only. The member properties to be applied in Equation (1) were obtained from material tests. As shown in Table 5, experimental axial strength P_{exp} was between P_{cri} and P_{crd}. It was more than 50 times larger than P_e. Thus, the buckling prevention effects of glulam timber were confirmed.

$$P_{cri} = \frac{\pi^2 EI_i}{L^2}, \quad P_{crd} = \frac{\pi^2 EI_d}{L^2}, \quad P_e = \frac{\pi^2 E_S I_S}{L^2} \tag{1}$$

Table 3 Specimens for Axial Compression Tests

Name	Steel Plate PL-t_s x b_s	Cedar-Glulam-Timber 2▯h_w x b_w	Number of (Glulam-Timber)-(Steel Plate) Joint	Number of Connectors at One Joint	Distance between each Joint *lc*
No.1 ⅣB h_w120c1x1	PL-16x180	2▯120x200	4	1	1500
No.2 ⅣB h_w150c1x1		2▯150x200			
No.3 ⅣB r150h_w120c2x1	PL-16x320	2▯120x350		2	
No.4 Ⅲ r150h_w120c2x1			3		2250
No.5 ⅣB r200h_w150c2x1	PL-22x420	2▯150x450	4		1500

Table 4 Mechanical Property of Steel Plate

Steel Plate				
Thickness mm	Yield Strength N/mm²	Tension Strength N/mm²	Elastic Coefficient (E_S) N/mm²(x10⁵)	Strain %
16	304	469	1.94	30.8
22	372	547	2.12	24.8

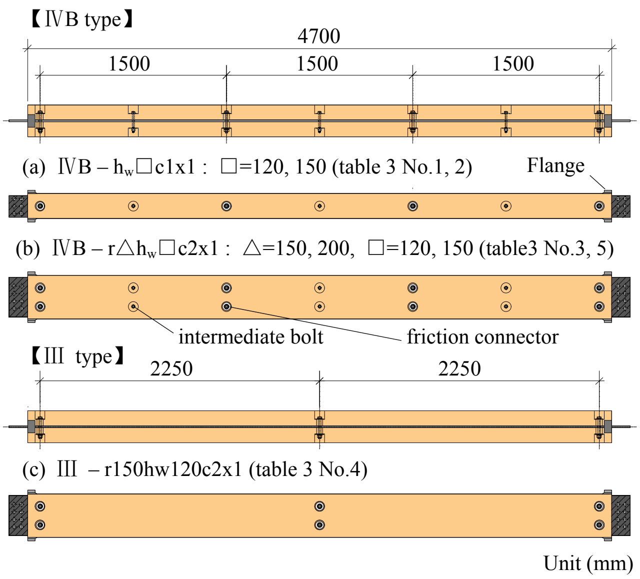

Figure 8 Specimens of Axial Compression Tests

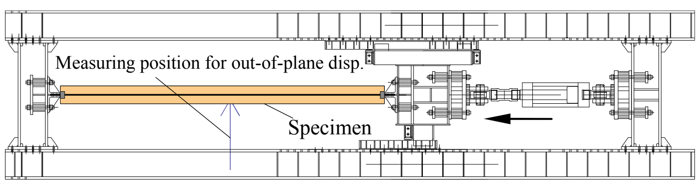

Figure 9 Test Apparatus of Axial Compression Tests

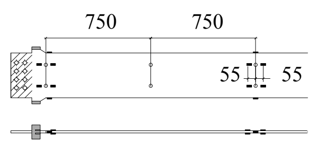

Figure 10 Location of Strain Gauges (Steel Plate)

where,

$$\left.\begin{aligned} EI_i &= 2\cdot E_{w_{y-y}} I_{wd} + E_s I_s + E_{w_{y-y}} A_w \frac{e^2}{2}, \quad EI_d = 2\cdot E_{w_{y-y}} I_{wd} + E_s I_s \\ I_{wd} &= \frac{b_w\cdot h_w{}^3}{12}, \quad I_s = \frac{b_s\cdot t_s{}^3}{12}, \quad A_w = b_w\cdot h_w, \quad A_s = b_s\cdot t_s, \quad e = h_w + t_s \end{aligned}\right\} \tag{2}$$

E_S: Yong's modulus of steel plate, $E_{Wy\text{-}y}$: bending Yong's modulus of glulam timber, t_S: thickness of steel plate, b_S: width of steel plate, h_W: thickness of glulam timber, b_W: width of glulam timber, and L: buckling length (= length of specimen)

Figure 11 shows axial force-axial deformation. Elastic stiffness K_s of steel plate only, and elastic coefficient K_{w+s} when steel plate and glulam timber are regarded having integrity. Each elastic stiffness was estimated using Equation (3).

$$K_s = \frac{E_s\cdot A_s}{L}, \quad K_w = \frac{E_{w_{y-y}}\cdot A_w}{L}, \quad K_{w+s} = K_s + 2K_w \tag{3}$$

As shown in Figure 11, all of the specimens showed that the initial stiffness was the same as K_{w+s}. Until axial strength was reached, only IVB-h_w150c1 showed gradually decreasing stiffness, while axial force increased above 500kN. The other four test pieces showed stiffnesses as high as K_{w+s} until axial strength was reached. Also, all of the specimens showed sustained axial strength after out-of-plane deformation progressed to some extent, as shown in Figure 12.

3.3.2 Failure of specimen

As shown in Figure 13, failure characteristics due to total buckling were confirmed in all of the specimens. The glulam timber on the tensile side showed cracking in IVB-h_w150c1 and IVB-r150h_w120c2. Cracking of the specimens both occurred at the connection location, showing cross-section damage of the glulam timber (Figure 13(b) and (c)). The rapid decrease in the load shown in Figures 11(b) and (c) was due to this cracking.

Table 5 Result of Axial Compression Tests of Hybrid Member

(Unit of Load is kN)

Name		P_{exp}	Buckling Mode	P_{cri}	P_{crd}	P_e	P_{exp}/P_{cri}	P_{exp}/P_e
ⅣB	h_w120c1	562	Total Backling	881	186	5.3	0.64	106
ⅣB	h_w150c1	721	Total Backling	1652	358	5.3	0.44	135
ⅣB	r150h_w120c2	935	Total Backling	1542	325	9.5	0.61	98.8
Ⅲ	r150h_w120c2	795	Total Backling	1542	325	9.5	0.52	84.0
ⅣB	r200h_w150c2	1845	Total Backling	3955	828	35.3	0.47	52.3

P_{exp} : Experimental result of maximum strength (= P_{max} in Fig. 11)
P_{cri} : Euler buckling strength when two glulam timbers and steel plate are combined entirely
P_{crd} : Euler buckling strength when two glulam timbers and steel plate are combined differently
P_e : Euler buckling strength of steel plate
※ Buckling mode is defined by objection

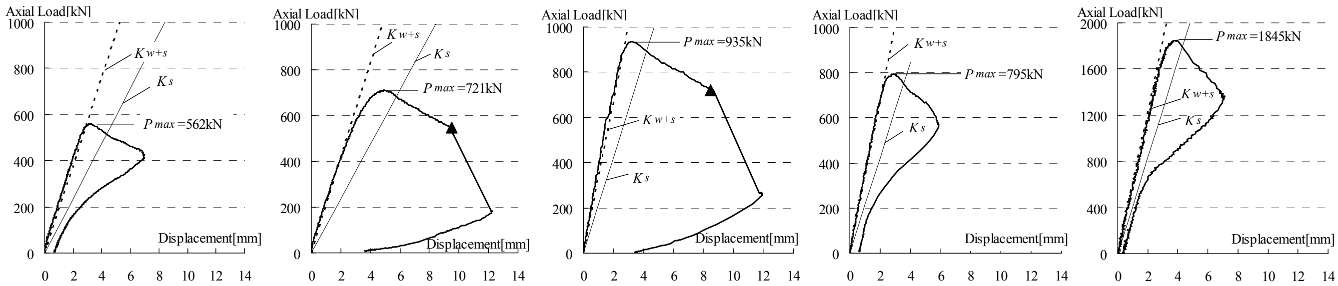

(a) ⅣB-h_w120c1x1 (b) ⅣB-h_w150c1x1 (c) ⅣB-r150h_w120c2x1 (d) Ⅲ-r150h_w120c2x1 (e) ⅣB-r200h_w150c2x1

Figure 11 Relationship Between Axial Force and Axial Deformation

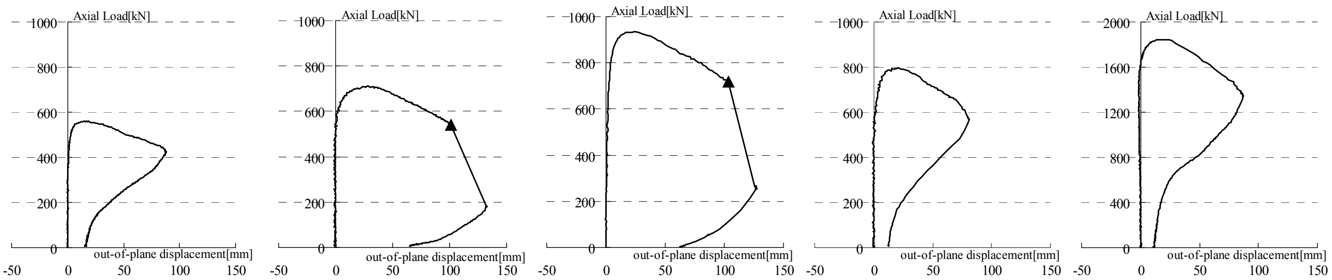

(a) ⅣB-h_w120c1x1 (b) ⅣB-h_w150c1x1 (c) ⅣB-r150h_w120c2x1 (d) Ⅲ-r150h_w120c2x1 (e) ⅣB-r200h_w150c2x1

Figure 12 Relationship Between Axial Force and Out-of-Plane Displacement at The Member Center

3.3.3 Distribution of axial force

The distribution of axial force borne by the steel plate, shown in Figure 14, refers to the state when the axial force was about half of the experimental axial strength P_{exp}. This was estimated from strain gauges (Figure 10) attached to the steel plate. For all the specimens experimental axial force distribution showed that axial force greatly decreased at the connection location at the member end. However, a flat distribution was shown at the central location of the member. The axial force borne by the steel plate at the center of the member was about 60% of the total axial force borne by the hybrid member. Thus, it is considered that about the other 40% of the axial force was borne by the two sheets of glulam timber.

4. METHOD FOR EVALUATING AXIAL STRENGTH

4.1. Outline of The Methods for Evaluating Strength

The bending stiffness of the hybrid member is influenced by the shear deformation at the connection location and varies depending on the loading conditions and member locations. Then, as shown in the lower right of Figure 15, it is assumed that glulam timber and steel plate would both contribute to shear stiffness per unit length K. The connectors at the member ends would have averaged stiffness during application of compressive and tensile loads during the shear tests. The following three parameters were incorporated. The first was axial strength P_{TB}[3)] (Equations (4) through (7)) against total buckling, taking into account the integration degree of steel plate and glulam timber using shear stiffness K shown in Figure 15. The second was axial strength P_{LB} (Equations (8) through (10)) when local buckling occurred in the steel plate at the member end location, derived from Johnson's parabolic Equation[5)]. The third was axial force in the hybrid member P_{QC}[4)] when shear force at the member end location derived from spring model shown in Figure 17 became Q. Estimated strength was defined as the axial strength shown in Section 4.2, incorporating the above three parameters P_{TB}, P_{LB} and P_{QC}.

$$P_{TB} = \frac{9.6 EI_c}{L^2}, \quad EI_c = \mu EI_d \tag{4), (5}$$

$$\mu = \frac{EI_i}{EI_d + \dfrac{4E_{wy-y}A_w e^2}{K \cdot \alpha \cdot L^2}\left\{1 - \cosh\dfrac{\sqrt{K\alpha}L}{2} + \tanh\dfrac{\sqrt{K\alpha}L}{2}\sinh\dfrac{\sqrt{K\alpha}L}{2}\right\}} \tag{6}$$

$$\alpha = \frac{EI_i}{EI_d E_{w_{y-y}} A_w}, \quad \beta = \frac{e}{2EI_d}, \quad e = h_w + t_s \tag{7}$$

where, K: shear stiffness of contact surface of glulam timber and steel plate per unit length (See Figure 15).

$$P_{LB} = \sigma_{cr-j} \cdot A_s, \quad \sigma_{cr-j} = \left\{1 - 0.4\left(\frac{\lambda_s}{\Lambda_s}\right)^2\right\}\sigma_{ys} \quad \text{(Johnson parabolic equation}^{5)}\text{)} \tag{8), (9}$$

$$\lambda_s = \frac{L_{LB}}{i_s}, \quad \Lambda_s = \sqrt{\frac{\pi E_s^{\,2}}{0.6\sigma_{ys}}}, \quad i_s = \sqrt{\frac{I_s}{A_s}}, \quad A_s = b_s \cdot t_s \tag{10}$$

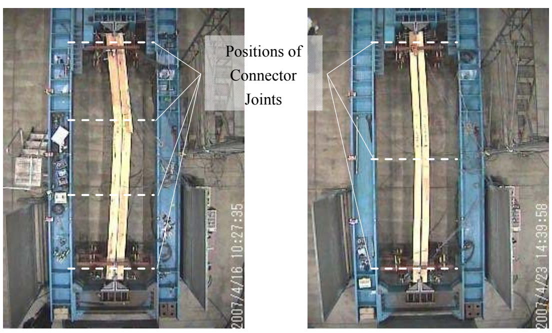

(a) ⅣB-h_w150c1 (b) Ⅲ-r150h_w120c2

Figure 13 Failure Characteristics after the Loading

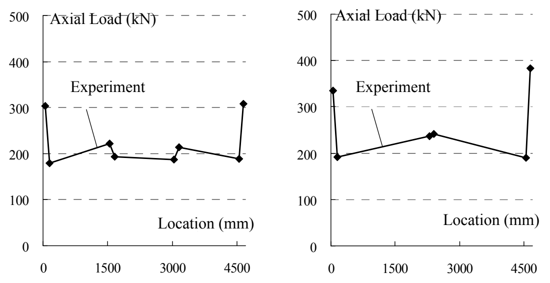

(a) ⅣB-h_w150c1 (b) Ⅲ-r150h_w120c2

Figure 14 Distribution of Axial Force on the Steel Plate
(When Axial Load is $P_{exp}/2$)

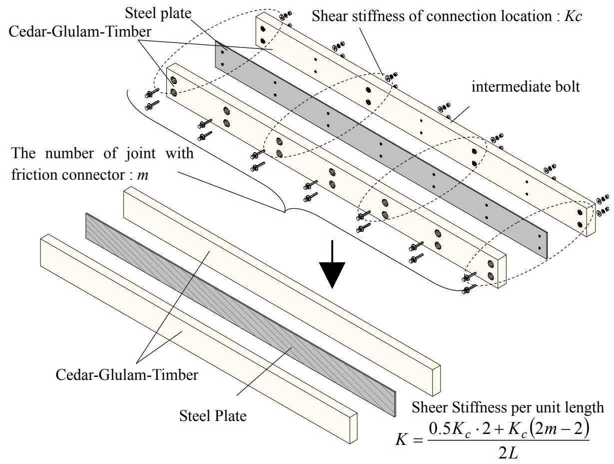

Figure 15 Hybrid Member

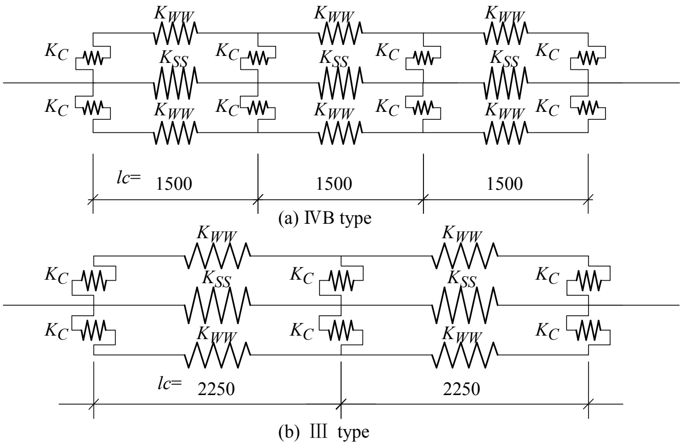

Figure 17 Spring Model of Hybrid Member

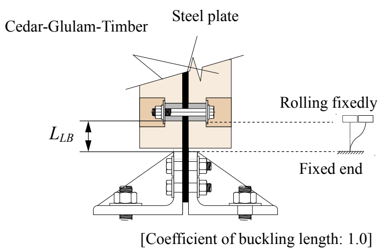

Figure 16 Boundary condition of member edge

Table 6 Stiffness of Spring in Figure 17

Specimen		Kc kN/mm	Kww kN/mm	Kss kN/mm
ⅣB	h_w120c1x1	Value of a variable	112	372
ⅣB	h_w150c1x1		140	372
ⅣB	r150h_w120c2x1		196	662
Ⅲ	r150h_w120c2x1		131	441
ⅣB	r200h_w150c2x1		315	1306

K_C : Shear stiffness of connection location (see Table 2)
K_{WW}: Axial stiffness of glulam timber from material property
K_{SS} : Axial stiffness of steel plate from material property

σ_{ys}: yield strength of steel plate, λ_s: slenderness ratio of steel plate, Λ_s: limit slenderness ratio of steel plate, L_{LB}: buckling length of steel plate

It is noted that P_{QC} changes with changing shear force borne by the connector, as shown in Figure 14, and changes with connector locations. However, shear stiffness K_c was assumed to be same at all connection locations, as shown in the spring model of Figure 17.

4.2. Applicability of Method to Strength Estimation

Results of the axial compression tests on the members and the relationship between P_{TB}, P_{LB} and P_{QC} are shown in Figure 18. The Y-axis and X-axis show the axial force in the hybrid member and the shear force Q of connectors, respectively. P_{TB} and P_{QC} were obtained by substituting shear stiffness K_c for shear force Q. Also, the estimation range was determined to be up to Q_{max}, where shear force Q became maximum. Table 7 shows the shear stiffness K_c at connection locations corresponding to each specimen. K_c is the shear stiffness existing at a single connection location. The bold line in Figure 18 shows the minimum P_{TB}, P_{LB} and P_{QC}, which change with shear force of connectors Q. ○ also shows the estimated axial strength.

Experimental results and estimated strength are compared in Table 8. The estimated figure for ⅣB-h_w150c1 was at about 14% lower than the experimental result (Figure 18(b)). The estimated figure for Ⅲ-r150h_w120c2 was 8% higher than the experimental result (Figure 18(d)). The estimated strengths generally agreed with the experimental results in all the test pieces, although some errors were found. Therefore, the method for estimating the strength described in Section 4.1 is considered applicable to cases for a hybrid member using friction connectors, such as where two connectors are used for a single connection location, and member cross-section is large. Regarding the failure characteristics, only ⅣB-h_w150c1 showed total buckling based on a visual check, as shown in Figure 18(b) and Table 8. However, axial strength was determined to be P_{QC} by the method for estimating the strength. This would be because the axial strength P_{TB} when total buckling occurred was very close to the axial strength P_{QC} when shear force reached Q_{max} at the connection location. The behavior where only ⅣB-h_w150c1 showed gradually decreasing stiffness before it reached axial strength would be related to the fact that shear force near Q_{max} was borne at the connector at the member end.

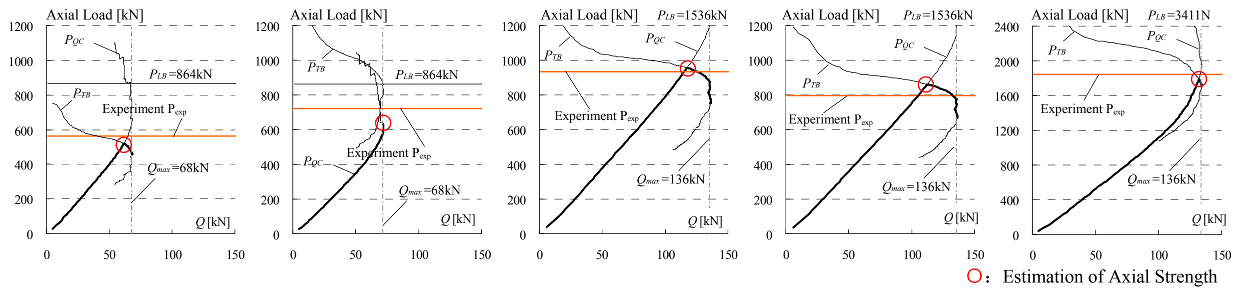

(a) ⅣB-h_w120c1x1 (b) ⅣB-h_w150c1x1 (c) ⅣB-r150h_w120c2x1 (d) Ⅲ-r150h_w120c2x1 (e) ⅣB-r200h_w150c2x1

Figure 18 Estimation of Axial Strength and Experimental Results

Table 7 Sheer Stiffness for Estimation of Axial Strength

Name		Shear stiffness of connection location: *Kc*	Reference Figure
ⅣB	h_w120c1x1	h_w120c1x1	Figure 7(a)
ⅣB	h_w150c1x1	h_w150c1x1	Figure 7(a)
ⅣB	r150h_w120c2x1	r150h_w120c2x1	Figure 7(b)
Ⅲ	r150h_w120c2x1	r150h_w120c2x1	Figure 7(b)
ⅣB	r200h_w150c2x1	r200h_w120c2x1	Figure 7(b)

Table 8 Estimation of Axial Strength and Experimental Results

Name		Maximum of Axial Load			Buckling Mode	
		Experiment *Pexp* [kN]	Estimation	Experiment / Estimation	Result	Methods for evaluating strength
ⅣB	h_w120c1x1	562	519	1.08	Total Buckling	Total Buckling
ⅣB	h_w150c1x1	721	630	1.14	Total Buckling	Reach Q_{max} at the connection
ⅣB	r150h_w120c2x1	935	956	0.98	Total Buckling	Total Buckling
Ⅲ	r150h_w120c2x1	795	860	0.92	Total Buckling	Total Buckling
ⅣB	r200h_w150c2x1	1845	1791	1.03	Total Buckling	Total Buckling

5. CONCLUDING REMARKS

Obtained findings are summarized as follows:

- It was confirmed that the friction connector had larger shear stiffness than the shear-ring connector.
- It was confirmed that shear stiffness and shear strength reached a ceiling when two connectors were placed in the member axial direction if the connector distance was over 200mm.
- c2x1 specimen, where two friction connectors were placed in the member axial-normal direction, showed about 1.8 times larger shear stiffness than the c1x1 specimen with a single connector.
- The initial stiffness of the hybrid member with a friction connector when it was subject to axial compression was the same as the stiffness of the unit body, if the glulam timber and steel plate were regarded having integrity.
- About 40% of the axial force borne by the hybrid member was borne by the two glulam timber plates in the friction connector.
- It was confirmed that the axial strength of the hybrid member with friction connectors could be estimated with high accuracy by adequately estimating the shear stiffness and strength of the friction connector.

REFERENCES

1) Suzuki, T., Sakata, H., Takeuchi, T., Matsuoka, Y., Nagayama, K. and Matsuda, K. (2005). Study on mechanical behavior of Glulam Timber-Steel composite member. Summaries of Technical Papers of Annual Meeting C1, 277-278

2) Sakata, H., Horii, T., Takeuchi, T., Nakamura, H. and Matsuda, K. (2008). Experimental study on shear performance of shear-ring connector. Journal of Structural and Construction Engineering 627:5, 773-779

3) Horii, T., Sakata, H., Takeuchi, T., Suzuki, T. and Nakamura, H. (2004). Experimental study on mechanical behavior of glulam timber steel composite member using shear-ring connector. Journal of Structural and Construction Engineering 584:10, 51-60

4) Sakata, H., Matsuda, K., Nakai, T., Takeuchi, T., Tomimoto, A., Nakamura, Y. and Nagayama, K. (2007). Study on Compressive Behavior of Glulam Timber-Steel Composite Member Adopted Friction Connector. Journal of Structural Engineering 53B:3, 323-328

5) (1996). Recommendations for Stability Design of Steel Structures, Architectural Institute of Japan

6) (2006). Standard for Structural Design of Timber Structures, Architectural Institute of Japan